Local Buckling and Crippling of Thin-Walled Composite Structures Under Axial Compression

A. D. Reddy,* L. W. Rehfield,† and R. I. Bruttomesso‡
Georgia Institute of Technology, Atlanta, Georgia
and
N. E. Krebs §
Sikorsky Aircraft, Stratford, Connecticut

The local buckling and crippling of thin-walled graphite/epoxy I-section beams under axial compression is investigated. The initial design of the specimens is based upon procedures used for metal structures. The specimen webs are manufactured from laminated woven graphite C3000 cloth with a 5225 resin system. Five ply layups—$(0)_{4s}$, $(45/0_2/45)_s$, $(0/45_2/0)_s$, $(0)_{3s}$, and $(45/0/45)_s$—are considered for the study. The specimens are compressively loaded to subcritical load levels and the critical loads are estimated using a stiffness plotting technique. They are loaded to failure subsequently. The NASTRAN code is used to predict the overall buckling behavior of the I-section. The correlation of the experimental and analytical results supports the validity of the design procedure.

Introduction

THE need for meeting the functional requirements in the present-day aircraft has necessitated use of composite materials in the airframe structure. These structures are normally designed with a stiffened construction for efficiency. Thus, stiffeners are part of these primary structures and constitute a significant portion of the total structural weight. When the stiffener is sturdy enough with respect to the skin, its axial, bending, and torsional stiffnesses provide elastic constraints to the skin element. In this case, only the general instability of the stiffened structure and the local buckling of the skin element are considered. On the other hand, if the stiffener is a short thin-walled structure, its members might buckle as plate elements locally in addition to the above modes.

A considerable amount of work has been done on local buckling of metallic stiffeners.[1-4] Consequently, there exist reliable design methods that are used routinely. The ability to design stiffeners of fiber-reinforced composite materials depends on the availability of reliable design procedures and a data base of test results. The amount of published work in this area is very limited.[5-7] There is a need for a data base and greater understanding of the local buckling behavior and subsequent crippling failure of these structural members.

In view of these observations, this effort has been undertaken. It is a continuation of earlier work done at Sikorsky Aircraft with angle sections fabricated from woven cloth. The I-section specimens considered here extend this earlier work by including stiffener elements that have both free edges and edges supported by contiguous neighbors to provide element boundary conditions. The main objectives are to 1) design the specimens using the existing procedures and validate them using the experimental data base generated on the buckling behavior, 2) understand/predict the interaction of elements, and 3) provide insight into the crippling failure process for this type of structure.

This paper presents the design procedure for the initial sizing of the specimens, experimental procedures, analytical results, and their correlation with the experimental data.

Specimen Design and Preparation

Design

The initial sizing of specimen was based on the design chart provided in Ref. 2. The material system selected was woven graphite C3000 cloth impregnated with an epoxy 5225 system. The typical material properties are listed in Table 1. The five ply layups—$(0)_4$, $(45/0_2/45)_s$, $(0/45_2/0)_s$, $(0)_{3s}$, and $(45/0/45)_s$—considered for the web are representative of some common layups used by Sikorsky Aircraft. They are coded as specimen types A–E, respectively. Also, the second and third layups are quasi-isotropic, the fourth is a fiber-dominated layup, and the

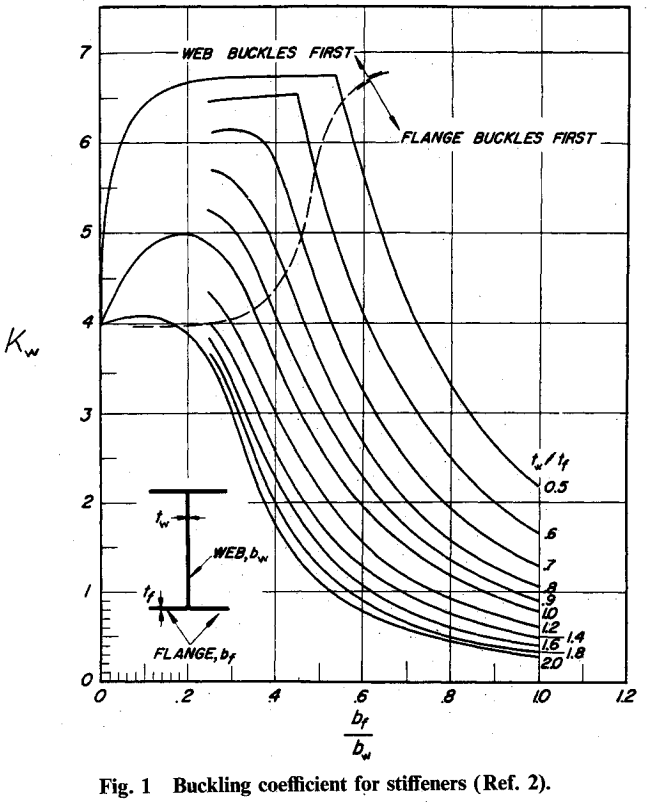

Fig. 1 Buckling coefficient for stiffeners (Ref. 2).

Received April 11, 1986; presented as Paper 85-0672 at the AIAA/ASME/ASCE/AHS 27th Structures, Structural Dynamics and Materials Conference, Orlando, FL, April 15–17, 1985; revision received Feb. 20, 1987.

*Senior Research Engineer, Department of Aerospace Engineering; presently Specialist Engineer, Lockheed-Georgia Company, Marietta, GA. Member AIAA.

†Professor, Department of Aerospace Engineering. Associate Fellow AIAA.

‡Graduate Research Assistant, Department of Aerospace Engineering.

§Structural Methods Development Engineer, Airframe Structures.

last is representative of the matrix-dominated layup. The overall properties of the laminates obtained with a laminated plate code are provided in Table 2. In Table 2, E_x and E_y are Young's moduli in the longitudinal and transverse directions, G_{xy} the shear modulus, v_{xy} the Poisson's ratio, A_{11}, A_{22}, A_{12}, A_{66} the laminate extensional stiffnesses, and D_{11}, D_{12}, D_{22}, D_{66} the laminate bending stiffnesses. As all the laminates are symmetric, the laminate coupling stiffnesses B_{ij} are all zero.

The design chart provided in Ref. 2 was used, together with the expression for critical stress, to select the widths of the flange and web. This chart is provided in Fig. 1 for convenience. For the same thickness for web and flanges, a flange-to-web width ratio of 1/4 was chosen to precipitate web buckling first. Then, the width of the flange and web were computed such that the resulting critical stresses were lower than the computed laminate ultimate stress values. This chart was used with the realization that this type of procedure is applicable to isotropic materials only. The resulting cross section of the specimen is shown in Fig. 2.

In order to select the length of the specimen, an anisotropic plate analysis code was used to compute the critical stress values for different web length-to-depth ratios. As the specimen was intended to be fabricated with encapsulated ends, clamped boundary conditions were imposed at the ends. Two cases were studied with the web edges clamped and simply supported. The range of web lengths chosen was to prevent Euler-type overall column buckling. The data on a plate with $(0)_{4s}$, layup is presented in Fig. 3. A length-to-depth ratio of 3 was chosen for all of the specimens uniformly from these data, with the worst case (clamped edge) critical stress below the ultimate stress. Also, three waves will minimize the end boundary condition effects.

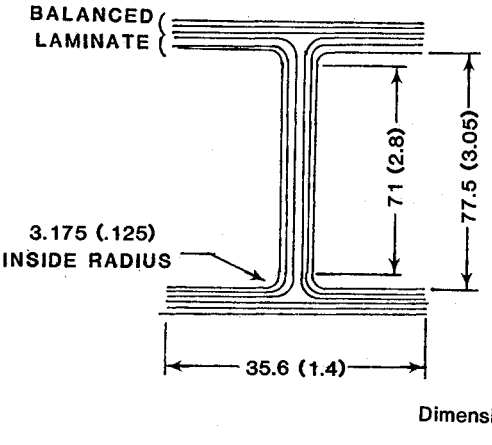

Fig. 2 Typical section of the specimen.

Table 1 Material properties of C3000/5225 graphite/epoxy woven cloth-design

E_{11} 10^6 psi	9.4	v_{12}	0.05
E_{22} 10^6 psi	9.4	F_{1c} ksi	85
G_{12} 10^6 psi	0.84	F_{2c} ksi	85

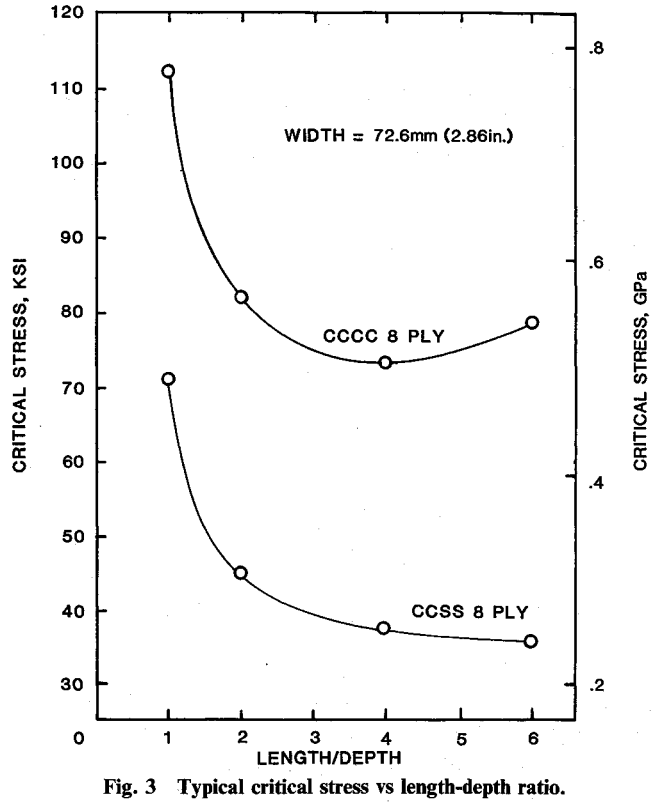

Fig. 3 Typical critical stress vs length-depth ratio.

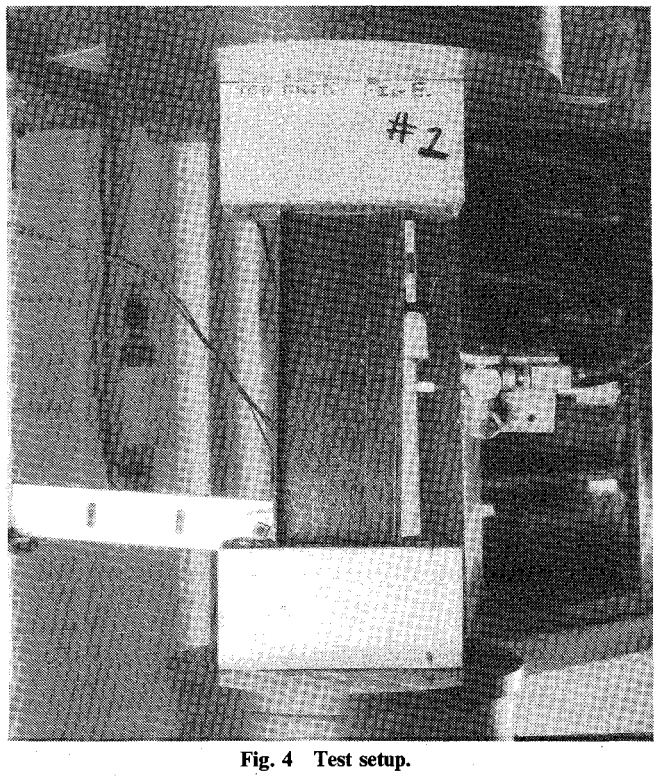

Fig. 4 Test setup.

Table 2 Estimated layup properties of specimens

Specimen type	Layup: Web	Layup: Flange	$E_{xx}=E_{yy}$, 10^6 psi	v_{xy}	G_{xy}, 10^6 psi	F_{c11}, ksi	A_{11}, 10^6/lb/in.	A_{12}, 10^6/lb/in.	A_{66}, 10^6 lb/in.	$D_{11}=D_{22}$, lb. in.	D_{12}, lb. in.	D_{66}, lb. in.
A	$(0)_{4s}$	$(0)_{4s}$	9.4	0.050	0.840	84.9	1.13	0.0565	0.1008	1357	68	121
B	$(45/0_2/45)_s$	$(45/0_2/45/0_4)_T$	6.92	0.300	2.658	57.9	0.913	0.2747	0.3189	1046	379	432
C	$(0/45_2/0)_s$	$(0/45_2/0_5)_T$	6.92	0.300	2.658	57.9	0.913	0.2747	0.3189	1144	281	334
D	$(0)_{3s}$	$(0)_{3s}$	9.4	0.050	0.84	84.9	0.848	0.0424	0.0756	572	29	51
E	$(45/0/45)_s$	$(45/0/45/0_3)_T$	5.8	0.414	3.264	46.4	0.623	0.2606	0.2937	409	192	215

Fabrication

The specimens were fabricated at Sikorsky Aircraft using a cocuring process. The web was sewed near the flange to prevent delamination along its midplane. This was done by using a Kevlar thread running stitch with 7 stitches/in. The selection of thread size and stitch frequency was based on the machine capability, final strength requirements of the product, and recommendations appearing in Ref. 8. At least three specimens of each type were fabricated for evaluation. These specimens were geometrically characterized before testing. The detailed average dimensions are presented in Table 3.

Experimental Program

The three types of tests performed on these specimens are explained in this section.

Initial Buckling Tests

In these tests, the specimens were loaded to subcritical load values in order to determine the initial buckling loads of the flange and the web separately. The specimens were mounted with back-to-back strain gages and linear variable differential transformer (LVDT) displacement transducers at appropriate locations to measure specimen strains, out-of-plane displacements, and overall end shortening. A typical test setup is shown in Fig. 4. The critical buckling load was determined nondestructively from these data using a stiffness plotting technique (Donnell plot). A typical plot is presented in Fig. 5 and the buckling load data summarized in Table 4.

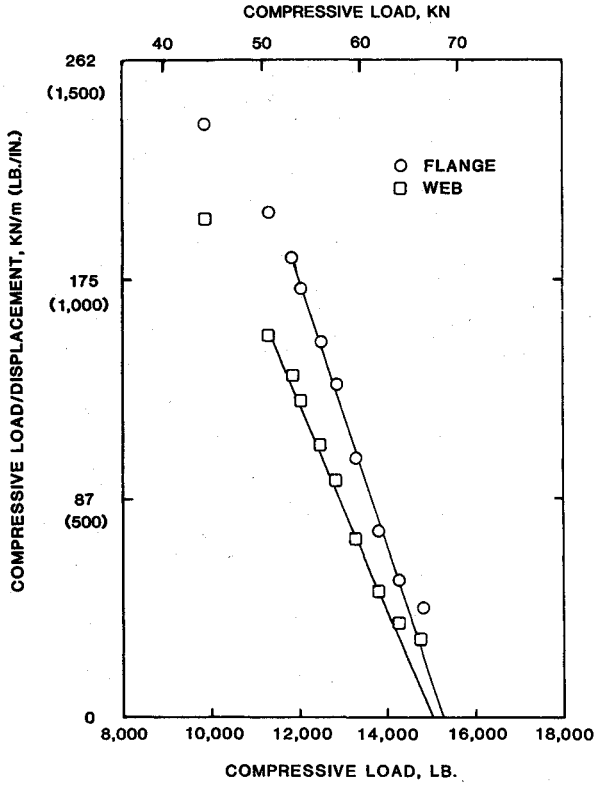

Fig. 5 Typical stiffness plot.

Postbuckling Tests

After obtaining consistent estimates of the critical loads from the above tests, the specimens were loaded into the postbuckling regime. The information sought here was on the initial postbuckling stiffness, which is an indicator of the interaction of section elements in the postbuckled range, the postbuckling or crippling strength, strains, and corresponding modes. The out-of-plane displacement and strain data in the postbuckling range were used to countercheck the initial buckling load data generated previously. The total load carried by a structure in the postbuckled regime can be expressed as the sum of two terms, one representing the critical load and the second a function of the square of the amplitude of the out-of-plane displacement. Consequently, the initial buckling load is estimated from the initial postbuckled test data by calculating the load axis intercept of the load vs the square of the out-of-

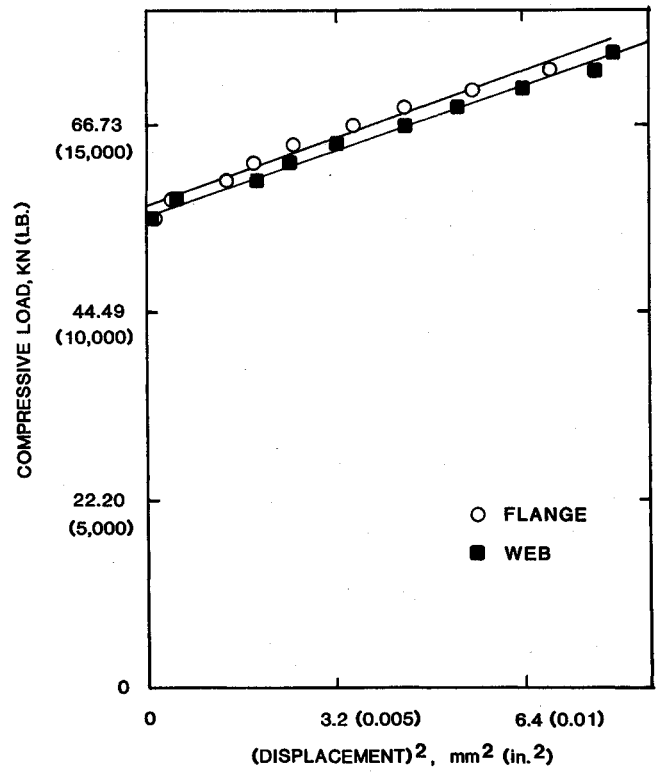

Fig. 6 Typical load vs (displacement)^2 plot.

Table 4 Summary of buckling test results

Specimen type	Buckling load, KN/m (lb/in.)	
	Web	Flange
A	670 (3828)	695 (3974)
B	833 (4759)	837 (4786)
C	849 (4856)	844 (4826)
D	289 (1651)	289 (1651)
E	391 (2235)	396 (2266)

Table 3 Typical specimen dimensions

Specimen type	Length, mm (in.)	Depth, mm (in.)		Thickness, mm (in.)	
		Web	Flange	Web	Flange
A	221 (8.716)	80 (3.1625)	38 (1.501)	3.2 (0.1257)	3 (0.1185)
B	217 (8.55)	80 (3.144)	35 (1.390)	3.2 (0.1280)	3 (0.1195)
C	209 (8.24)	80 (3.166)	35 (1.383)	3.3 (0.1297)	3.1 (0.121)
D	214 (8.44)	80 (3.170)	37 (1.444)	2.3 (0.0927)	2.3 (0.09)
E	215 (8.48)	79 (3.123)	37 (1.450)	2.3 (0.0922)	2.2 (0.087)

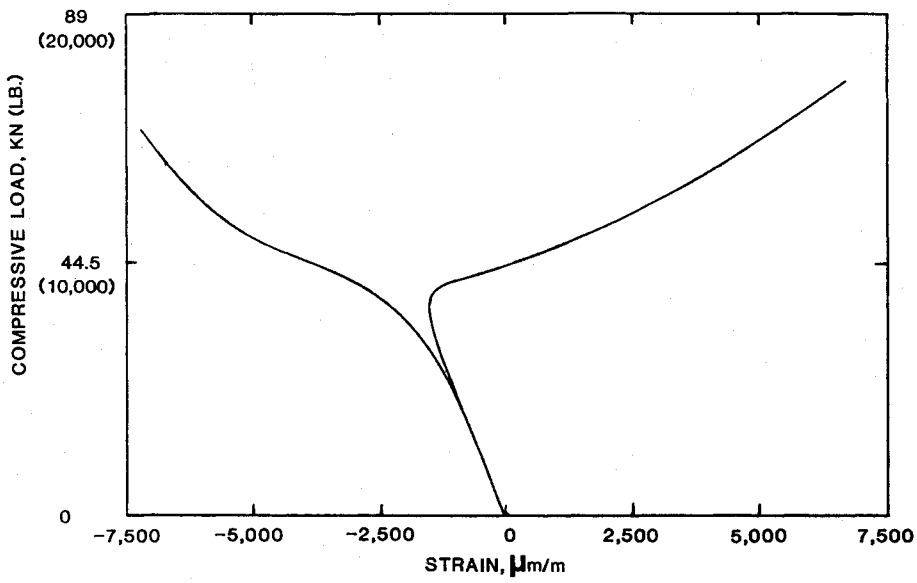

Fig. 7 Typical load vs strain plot.

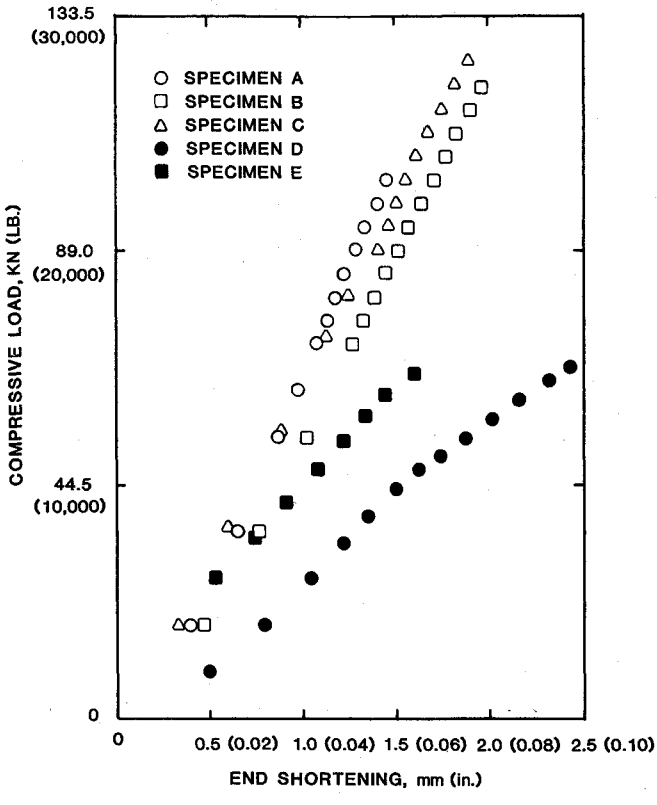

Fig. 8 Initial postbuckling test results.

Table 5 Summary of postbuckling test results

Specimen type	Initial postbuckled stiffness, KN/m (lb/in.)	Crippling load, KN/m (lb/in.)
A	30645 (175,180)	780 (4461)
B	49697 (284,091)	915 (5233)
C	31767 (181,594)	880 (5030)
D	21867 (125,000)	502 (2872)
E	25238 (144,270)	456 (2607)

plane displacement plot (Fig. 6). These estimates are further substantiated by locating the point of strain divergence in the load-strain plot (Fig. 7).

The initial postbuckling stiffness data generated using Fig. 8 and the crippling loads are presented in Table 5. Figure 9

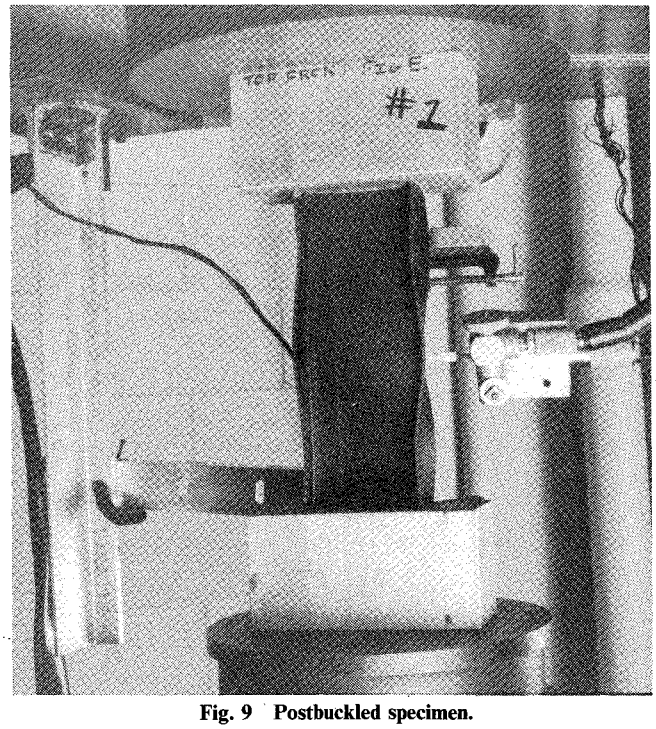

Fig. 9 Postbuckled specimen.

shows the postbuckled specimen before failure; three buckle waves can be clearly seen. Figure 10 shows the crippled specimen.

Material Characterization Tests

The failure site on all the specimens was at the crest of the buckle wave close to the end (Fig. 9). This facilitated two types of specimens to be generated from the specimens failed in the postbuckled tests. One was a beam specimen of the laminate cut out from the web area of the I-section and the other a short compression test specimen of the thin-walled compression member (I-section) itself. A three-point bend test was performed on the beam specimen to determine the actual Young's modulus of the web material in flexure. The short compression test specimens were instrumented in the center of the web with back-to-back strain gages and loaded until failure. The results of these tests are summarized in Table 6. A compression test load-strain history is presented in Fig. 11.

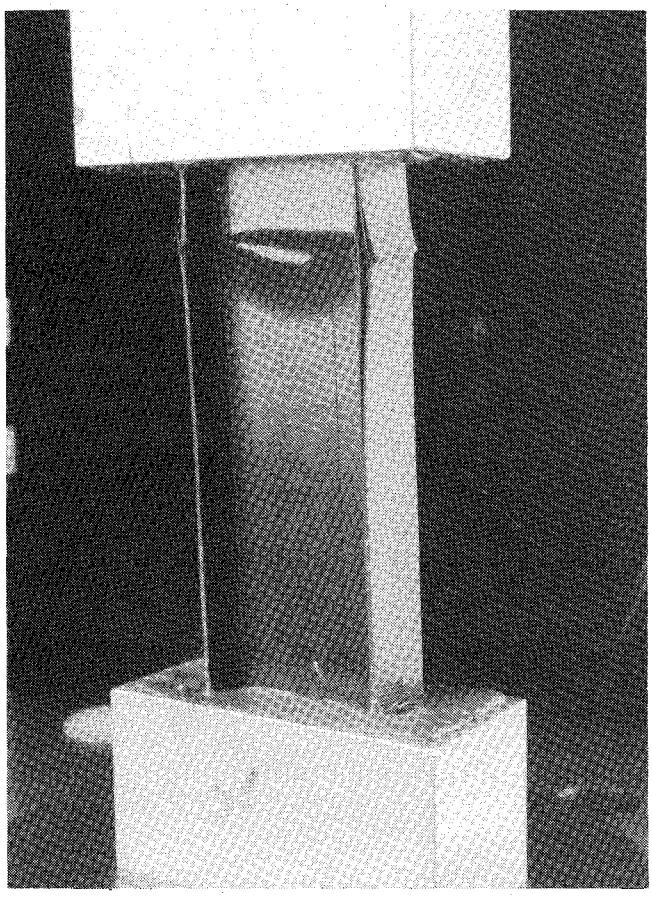

Fig. 10 Crippled specimen.

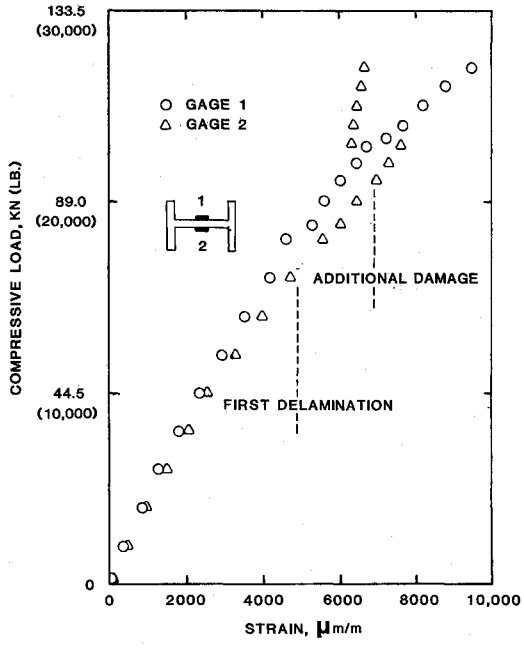

Fig. 11 Load vs strain—ultimate compression test.

Table 6 Summary of material characterization test results

Specimen type	Estimated Young's modulus GPa(10^6 psi)	Ultimate load KN/m (lb/in.)
A	47.97 (6.96)	1064 (6083)
B	36.25 (5.26)	931 (5323)
C	36.25 (5.26)	1047 (5985)
D	43.28 (6.28)	949 (5427)
E	35.28 (5.12)	784 (4483)

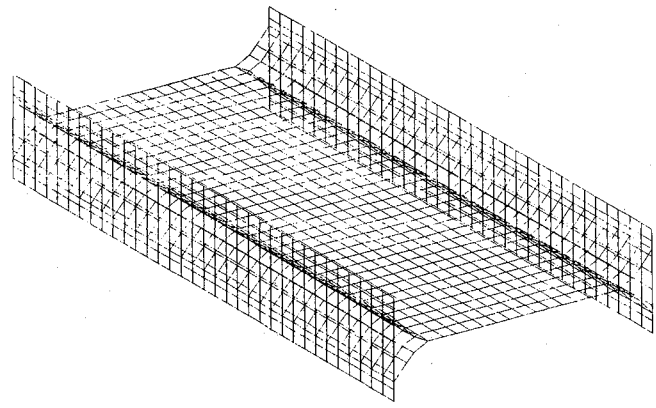

Fig. 12 Finite-element model of the specimen.

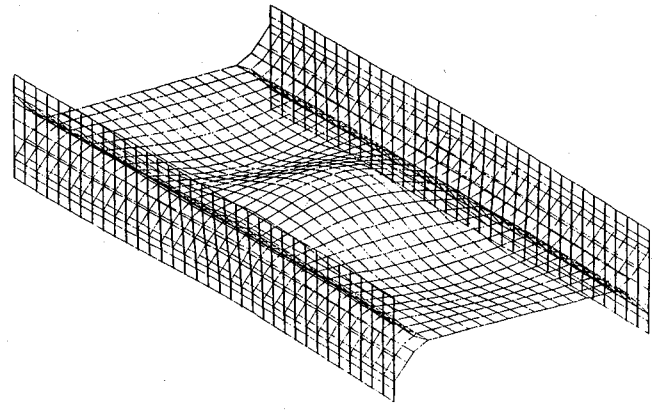

Fig. 13 Typical deformed configuration of the specimen.

Table 7 Buckling load results—NASTRAN

Specimen type	Buckling load, KN/m (lb/in.) Web	Flange
A	557 (3186)	573 (3275)
B	796 (4550)	796 (4550)
C	773 (4420)	791 (4522)
D	229 (1308)	229 (1308)
E	410 (2344)	410 (2344)

Table 8 Summary of strain data from failure tests

Specimen type	Maximum strain, μm/m Postbuckling failure	Compression failure
A	−11068	—
B	−8764	−8174
C	−6168[a]	−7699
D	−12532	−9824
E	—	−9500

[a]Data from gage mounted away from the failure site, close to the center of the specimen.

Analysis

The analysis was carried out using the NASTRAN program. The model was created by using the 1496 quadrilateral plate elements as shown in Fig. 12. The buckled configuration under uniaxial compression is presented in Fig. 13 and the load values are listed in Table 7. These predictions use the measured specimen flexural stiffnesses and the nominal design dimensions.

Discussion of Results

Comparison of the buckling load data in Table 4 with the ultimate load from the compression test in Table 6 shows that

the specimens buckled at a lower load value than the ultimate value, as designed. Also, the experimental buckling load results in Table 4 on the web and flange support the critical design requirement for the web to buckle first. Although not separated by a wide margin, the web buckles before the flange in all cases except for specimen C. These results thus support the adequacy of the preliminary design procedures adopted.

The crippling load data presented in Table 5 show that only specimen type D has the highest postbuckling load capability, the ratio of the buckling load to the crippling load being equal to 1.74. The compression test specimen is designed to prevent buckling and the strain value obtained from this test is the maximum this structure can take before failure. Although the closeness of strain data in Table 8 suggests some correspondence between the postbuckling failure (crippling) and short-column compression failure processes, delamination of the flange at the free edge (Fig. 11) seems to be the initiator of the failure in the later type of tests.

The comparison of the experimental and NASTRAN buckling load values on the web and flange suggest that the modeling is good and can predict the overall behavior of the thin-walled member very well when the actual geometric and material properties are input.

Conclusions

The results support the design approach used and the specimen behaves as designed. The NASTRAN predictions correlate well with the test data.

Acknowledgments

This work was supported under U.S. Army Research Office Contract DAAG 29-82-K-0094 and by Sikorsky Aircraft. This support is gratefully acknowledged.

References

[1]Gerard, G. and Becker, H., "Handbook of Structural Stability, Part I—Buckling of Flat Plates," NACA TN 3781, 1957.

[2]Becker, H., "Handbook of Structural Stability, Part II—Buckling of Composite Elements," NACA TN 3782, 1957.

[3]Gerard G., "Handbook of Structural Stability, Part IV—Failure of Plates and Composite Elements," NACA TN 3784, 1957.

[4]Bruhn, E. F., "Analysis and Design of Flight Vehicle Structures," S. R. Jacobs and Associates, Indianapolis, IN, June 1973.

[5]Spier, E. E., "Crippling/Column Buckling Analysis and Test of Graphite/Epoxy Stiffened Panels," *Proceedings of the 16th AIAA/ASME/SAE Structural Dynamics and Materials Conference,* AIAA, New York, Vol. 1, 1975, pp. 1-15.

[6]Spier, E. E. and Klouman, F. L., "Empirical Crippling Analysis of Graphite/Epoxy Laminated Plates," *Composite Materials; Testing and Design (Fourth Conference)* STP 617, American Society for Testing and Materials, Philadelphia, 1977, pp. 255–271.

[7]Renieri, M. P. and Garrett, R. A., "Investigation of the Local Buckling, Postbuckling and Crippling Behavior of Graphite/Epoxy Short Thin Walled Compression Members," McDonnell Douglas Aircraft Co., St. Louis, MDC A7091, July 1981.

[8]Holt, D. J., "Future Composite Aircraft Struct6ures May be Sewn Together," Society of Automotive Engineers Paper 82, 1982.

[9]Horton, W. H., Cundari, F. L., and Johnson, B. W., "Applicability of Southwell Plot to the Interpretation of Test Data Obtained from Stability Studies of Elastic Column and Plate Structures," USAAVLABS Tech. Rept. 69-32, Nov. 1976.